Received 2 September 2022; accepted 20 September 2022. Date of publication 27 September 2022; date of current version 6 October 2022.

Digital Object Identifier 10.1109/OJCOMS.2022.3209952

Impact of Antenna Distribution on Spectral and Energy Efficiency of Cell-Free Massive MIMO With Transmit Power Control Algorithms

MASAAKI ITO [1,2], ISSEI KANNO [1], KOSUKE YAMAZAKI [1], YOJI KISHI [1], WEI-YU CHEN [2], THOMAS CHOI [2] (Graduate Student Member, IEEE), AND ANDREAS F. MOLISCH [2] (Fellow, IEEE)

[1]Wireless Technology Division, KDDI Research, Inc., Fujimino 3568502, Saitama, Japan

[2]Ming Hsieh Department of Electrical and Computer Engineering, University of Southern California, Los Angeles, CA 90089, USA

CORRESPONDING AUTHOR: M. ITO (e-mail: sk-itou@kddi.com)

Parts of this work were presented at 2021 IEEE 94th Vehicular Technology Conference [15] [DOI: 10.1109/VTC2021-Fall52928.2021.9625300] and 2021 IEEE GLOBECOM Workshops [24] [DOI: 10.1109/GCWkshps52748.2021.9682135].

ABSTRACT Cell-free massive multiple-input multiple-output (CF-mMIMO) systems are expected to provide faster and more robust connections to user equipments by cooperation of a massive number of distributed access points (APs), and to be one of the key technologies for beyond 5G (B5G). CF-mMIMO systems with multiple-antenna APs have been investigated from various viewpoints recently. However, no comprehensive analysis of the impact of antenna distribution on CF-mMIMO system performance has been done so far, which is important for practical deployment. Besides spectral efficiency, in B5G, energy efficiency of user equipments is one of the key indicators because various kinds of battery-limited devices connect to the network. Thus, this paper provides a comprehensive performance analysis of the impact of antenna distribution on the performance indicators, while considering several combining/precoding schemes and transmit power control algorithms. For uplink maximal-ratio combining, the concentrated deployment has the best performance thanks to the channel hardening and favorable propagation phenomena. On the other hand, the concentrated deployment prominently suffers from shadowing effects. For uplink/downlink minimum mean-square error combining with transmit power control, the semi-distributed deployments show the best performance, and it implies that we can reduce the number of APs to 1/4 for uplink and to 1/2 for downlink while keeping the same performance as the fully-distributed deployment.

INDEX TERMS Antenna distribution, battery lifetime prolongation, cell-free massive MIMO, energy efficiency, spectral efficiency, transmit power control.

I. INTRODUCTION

IN CONVENTIONAL cellular network systems, user equipments (UEs) in a certain area called cell are connected only to the base station. To improve UE performance in cellular systems, cells are deployed densely. However, the resulting inter-cell interference not only limits performance, but also causes unfair penalization of cell-edge UEs compared to the cell-center UEs [1]. To remedy these problems, cell-free massive multiple-input multiple-output (CF-mMIMO) eliminates the concept of cell [2], [3].[1] Access points (APs) are distributed in a network coverage area, and all APs cooperate with each other to enhance performance of all UEs; consequently all signals are "useful," and inter-cell interference is completely absent. In addition, the distance between an AP and a UE becomes shorter, which realizes better channel condition, especially for the "cell-edge" UEs in cellular systems, and provides macro-diversity against shadowing. Furthermore, every AP connects to the central processing unit (CPU), and the CPU conducts signal processing. CF-mMIMO will be an expected important technology for beyond 5G (B5G), or 6G,[2] because it improves performance and enables network operators

1. CF-mMIMO is also strongly related to the concepts of network MIMO, CoMP, and C-RAN.

2. The terms B5G, which we use henceforth, and 6G are used interchangeably in the literature.

to design networks more flexibly for various scenarios of B5G [4].

In B5G scenarios, there are two main performance indicators: spectral efficiency (SE) and energy efficiency (EE). Until now, many methods have been considered for (i) maximizing SE, i.e., to make the best use of the precious spectrum resource; this is also related to the user-experienced data rates, and (ii) maximizing the total EE of a network, and (iii) maximizing EE of each UE. Improvement of the total EE is important for environmental reasons, e.g., Sustainable Development Goals (SDGs), and to minimize electricity expenses of the operators, while the EE of each UE determines necessary battery capacity and/or the lifetime of a device, e.g., Internet of Things (IoT) [5], [6], [7]. As mentioned in the previous paragraph, CF-mMIMO can realize flexible optimization for both SE and EE.

When CF-mMIMO first appeared under this name around 2015 [8], [9], a default assumption for academic investigations was that each AP has a single antenna. Soon after that, multiple-antenna APs were also taken into account [10], [11], and this has become a common system model by now. Such multi-antenna APs are a more natural approach for improving UE performance while keeping the number of AP locations (which mostly determine deployment cost) constant. The antenna distribution has been investigated, e.g., in 5G networks [12]. Reference [13] investigates two key phenomena called channel hardening and favorable propagation on CF-mMIMO systems with maximal-ratio combining (MRC). It reveals that, for a given antenna density, it is beneficial to have a few multi-antenna APs rather than many single-antenna APs to harden channels. However, it does not clarify onto how many APs a given number of antennas should be distributed. This viewpoint is important especially for network operators. The superior performance of semi-distributed deployments (multiple-antenna APs) compared to the fully-distributed deployment (single-antenna APs) was also shown experimentally in an indoor environment [14]. However, the performance of CF-mMIMO in terms of AP antenna distribution has not been fully investigated yet. Reduction of number of APs has benefit especially for network operators. For example, one of the difficulties for system deployment is to acquire sites to install APs by buying or renting from others. If the semi-distributed case has better performance than the fully-distributed case, it makes it easier to deploy CF-mMIMO systems. In addition, reduction of number of APs makes the total length of wired fronthaul between APs and CPUs shorter and thus also reduces the cost. This paper aims at providing a general evaluation both uplink and downlink semi-distributed CF-mMIMO including several different combining (beamforming)[3]/precoding schemes and transmit power control (TPC) algorithms.

In a commercial operation, TPC is implemented to modify SE or EE with the goal of improvement of UE performance by reducing interference from neighboring UEs. Several TPC algorithms have been proposed; the most common algorithm in CF-mMIMO papers is to maximize the minimum SE among all UEs; for convenience, we henceforth refer to it as the max-min SE algorithm [2]. In our conference paper [15], we analyzed semi-distributed CF-mMIMO systems, including the impact of the max-min SE algorithms. It revealed the superiority of semi-distributed deployments for uplink zero-forcing (ZF), but the performance is still unclear for other combining schemes, e.g., MRC or minimum mean-square error (MMSE), downlink communications, the shadowing effects and TPC algorithms. Other proposed TPC algorithms focus on maximizing EE [16], [17], [18], [19]. However, those papers target the *total*, i.e., whole-network, EE. If total EE is focused on, some UEs can communicate with high EE and others may suffer from low EE, which causes the battery of the latter UEs to deplete more quickly.

As we assume that CF-mMIMO is deployed for one of the aforementioned B5G applications, improvement of each UE's EE is one of the key requirements to prolong a battery life. Therefore, investigation of TPC algorithms targeting maximization of each UE's EE is also important. In [20], [21], [22], [23], authors propose the maximization of the minimum EE as an optimization criterion, and evaluate its performance in conventional cellular systems, not in distributed antenna systems. The performance should be different in CF-mMIMO because the propagation characteristics is different from conventional cellular systems. Motivated by this, in [24], the authors investigated the performance of EE, especially focused on the minimum EE of UEs. We also obtained real-world channel data by using a drone, and evaluated their impact on performance by computer simulations [25], [26].

The contribution and findings of this paper are as follows:

- General investigation of the impact of antenna distribution on the performance of CF-mMIMO in the uplink and downlink. Numerical results are obtained with two common combining schemes (MRC and MMSE) as well as three TPC algorithms (max-min SE, maximizing the sum SE (max-sum SE), and maximizing the minimum EE (max-min EE)). Especially, the performance with the max-min EE algorithms in CF-mMIMO systems has not been investigated yet.
- Investigation of the outage probability[4] of EE per UE, which can be used as an indicator to evaluate whether UEs waste their batteries, with the combining schemes mentioned above. It is noteworthy that even though outage probability is one of the important indicators, previous works do not provide investigations for CF-mMIMO.

3. Both combining and beamforming are commonly used to denote the linear combination of antenna signals, and we will use "combining" hereinafter.

4. In this paper, outage probability means the probability that a performance threshold is not met. Actual values of threshold change depending on service requirements, and so do the outage probabilities.

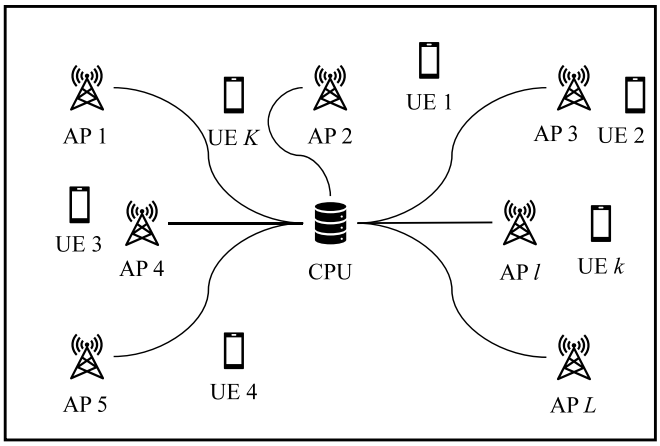

FIGURE 1. System model of CF-mMIMO where each UE communicates with all APs. We assume that every UE has a single antenna, and each AP may have multiple antennas. Each AP is connected to the CPU, which executes signal processing.

- Clarifying that, in uplink MRC, the concentrated deployment shows the best SE and EE performance on average. However, with the concentrated deployment, the performance of UEs suffering from bad channel condition is severely affected by shadowing effects. In this way, semi-distributed deployments have superiority.
- Clarifying that semi-distributed deployments outperform the fully-distributed and concentrated deployment in all cases for MMSE with TPC. This implies that network operators can reduce the cost of deployment for antenna distribution while keeping UE performance at a given level.

Notation is as follows: boldface lowercase and uppercase letters denote column vectors and matrices, respectively. Especially, $\mathbf{0}_{LN}$ denotes an all-zero vector with length of LN. The superscripts $(\cdot)^{\mathrm{T}}$, $(\cdot)^{\mathrm{H}}$, and $(\cdot)^{-1}$ denote the transposed matrix, the Hermitian transpose, and matrix inverse, respectively. The absolute value, the Euclidean norm of a vector, and the expectation are denoted by $|\cdot|$, $\|\cdot\|$, and $\mathbb{E}\{\cdot\}$, respectively. diag$\{\boldsymbol{x}\}$ denotes the transformation from a vector to a diagonal matrix, where the elements of a vector are allocated diagonally. Similarly, diag$\{\boldsymbol{X}\}$ denotes the transformation from a diagonal matrix to a vector, where the diagonal elements of a matrix are the elements of a vector. $\boldsymbol{X} \otimes \boldsymbol{Y}$ denotes Kronecker product of matrices, where each element is $x_{ab}\boldsymbol{Y}$. Finally, $z \sim \mathcal{N}_{\mathbb{C}}(0, 1)$ stands for a complex Gaussian random variable z with mean 0 and variance 1.

II. SYSTEM MODEL

There are L APs deployed in an area, and each AP is equipped with N antennas. Thus, the total number of AP antennas is LN. The index of the nth antenna of the lth AP antenna is expressed by using a tuple (l, n). Here, $L = 1$ means the concentrated deployment, and $N = 1$ means the fully-distributed deployment. All K UEs are spatially multiplexed in the area, and communicate with all APs. We assume that each UE has a single antenna. The system is illustrated in Fig. 1.

The channel coefficient (complex channel gain) $h_{l,n,k}$ between the (l, n)-th antenna and the kth UE can be modeled as

$$h_{l,n,k} = \sqrt{\beta_{l,k}} p_{l,n,k}, \tag{1}$$

where $\beta_{l,k}$ describes the path loss and large-scale power variations (shadowing) between the lth AP and the kth UE, and $p_{l,n,k}$ is the (complex) small-scale fading. The indexes of antennas ((l, n)) and APs (l) are used in (1) to analyze the relationship between performance results and antenna distribution, which is discussed in Section V.

More specific channels are explained in the following by dividing the channel into line-of-sight (LoS) and non-line-of-sight (NLoS) components. We assume throughout the paper that the channel is frequency-non-selective and time-invariant over the duration of transmission. Generalization to the frequency-selective case are straightforward assuming that OFDM is used as modulation format.

A LoS channel vector $\boldsymbol{h}_k^{(\mathrm{LoS})} \in \mathbb{C}^{LN \times 1}$ for the kth UE is given as follows:

$$\boldsymbol{h}_k^{(\mathrm{LoS})} = \underbrace{\begin{bmatrix} \boldsymbol{B}_{1,k} & \cdots & 0 \\ \vdots & \ddots & \vdots \\ 0 & \cdots & \boldsymbol{B}_{L,k} \end{bmatrix}}_{\boldsymbol{B}_k} \begin{bmatrix} \boldsymbol{p}_{1,k}^{(\mathrm{LoS})} \\ \vdots \\ \boldsymbol{p}_{L,k}^{(\mathrm{LoS})} \end{bmatrix}, \tag{2}$$

where $\boldsymbol{B}_{l,k} \in \mathbb{C}^{N \times N}$ is a diagonal matrix of large-scale fading, and $\boldsymbol{B}_k \in \mathbb{C}^{LN \times LN}$ is given by

$$\boldsymbol{B}_k = \mathrm{diag}\begin{bmatrix} \sqrt{\beta_{1,k}} \\ \vdots \\ \sqrt{\beta_{L,k}} \end{bmatrix} \otimes \boldsymbol{I}_N. \tag{3}$$

Note that large-scale fading coefficients correspond to each channel between an AP and a UE. $\boldsymbol{p}_{l,k}^{(\mathrm{LoS})} \in \mathbb{C}^{N \times 1}$ is a vector of local phase changes of the LoS component within the lth AP.

Similarly, an NLoS channel vector $\boldsymbol{h}_k^{(\mathrm{NLoS})} \in \mathbb{C}^{LN \times 1}$ for the kth UE is given by

$$\boldsymbol{h}_k^{(\mathrm{NLoS})} = \boldsymbol{B}_k \boldsymbol{R}_k^{1/2} \boldsymbol{p}_k^{(\mathrm{NLoS})}, \tag{4}$$

where $\boldsymbol{R}_k \in \mathbb{C}^{LN \times LN}$ is a block diagonal small-scale fading correlation matrix denoted as

$$\boldsymbol{R}_k = \begin{bmatrix} \boldsymbol{R}_{1,k} & \cdots & 0 \\ \vdots & \ddots & \vdots \\ 0 & \cdots & \boldsymbol{R}_{L,k} \end{bmatrix}, \tag{5}$$

where the elements of the lth block depend on the angular power spectrum at the lth AP, and each element of $\boldsymbol{p}_k^{(\mathrm{NLoS})}$ is $\boldsymbol{p}_{l,k}^{(\mathrm{NLoS})} \in \mathbb{C}^{N \times 1} = \mathcal{N}_{\mathbb{C}}(0, 1)$.

Finally, the channel vector of Rician fading for the kth UE can be written by using diagonal matrices as

$$\boldsymbol{h}_k = \begin{bmatrix} \boldsymbol{F}_{1,k}^{(\mathrm{LoS})} & \cdots & 0 \\ \vdots & \ddots & \vdots \\ 0 & \cdots & \boldsymbol{F}_{L,k}^{(\mathrm{LoS})} \end{bmatrix} \boldsymbol{h}_k^{(\mathrm{LoS})} + \begin{bmatrix} \boldsymbol{F}_{1,k}^{(\mathrm{NLoS})} & \cdots & 0 \\ \vdots & \ddots & \vdots \\ 0 & \cdots & \boldsymbol{F}_{L,k}^{(\mathrm{NLoS})} \end{bmatrix} \boldsymbol{h}_k^{(\mathrm{NLoS})}, \quad (6)$$

where $\boldsymbol{F}_{l,k}^{(\mathrm{LoS})}, \boldsymbol{F}_{l,k}^{(\mathrm{NLoS})} \in \mathbb{R}^{N\times N}$ denote Rician K-factor matrices, and are expressed as

$$\boldsymbol{F}_{l,k}^{(\mathrm{LoS})} = \begin{bmatrix} \sqrt{\frac{\kappa_{l,k}}{\kappa_{l,k}+1}} & \cdots & 0 \\ \vdots & \ddots & \vdots \\ 0 & \cdots & \sqrt{\frac{\kappa_{l,k}}{\kappa_{l,k}+1}} \end{bmatrix}, \quad (7)$$

$$\boldsymbol{F}_{l,k}^{(\mathrm{NLoS})} = \begin{bmatrix} \sqrt{\frac{1}{\kappa_{l,k}+1}} & \cdots & 0 \\ \vdots & \ddots & \vdots \\ 0 & \cdots & \sqrt{\frac{1}{\kappa_{l,k}+1}} \end{bmatrix}. \quad (8)$$

$\kappa_{l,k}$ is the K-factor between the lth AP and the kth UE. We assume here implicitly that all antenna elements on an AP experience the same large-scale fading, shadowing, and Rician factor, which is fulfilled for a (reasonably small) uniform linear or rectangular array. In the parlance of the standardization organization 3GPP, we assume the antennas on an AP to be "co-located" [27].

A. UPLINK SIGNAL MODEL

The received signal at the (l, n)-th antenna of the ith symbol is given by

$$y_{l,n}(i) = \sqrt{\rho^{(\mathrm{u})}} \sum_{k=1}^{K} h_{l,n,k}\sqrt{q_k} s_k(i) + z_{l,n}(i), \quad (9)$$

where $s_k(i)$ is a transmitted symbol of the kth UE normalized to unit average power, and its transmit power coefficient is q_k, i.e., the maximum value is 1. $z_{l,n}(i) \sim \mathcal{N}_{\mathbb{C}}(0, 1)$ is the normalized additive white Gaussian noise (AWGN) at the (l, n)-th antenna. $\rho^{(\mathrm{u})}$ is the transmit signal-to-noise ratio (SNR), i.e., the ratio of the maximum transmitted signal power divided by the noise power.

B. CHANNEL ESTIMATION

For channel estimation, $\tau^{(\mathrm{p})}$ pilot resources are allocated within the coherence interval, and all UEs transmit pilot signals in the resources. Let $\sqrt{\tau^{(\mathrm{p})}}\boldsymbol{\varphi}_k$ be the $\tau^{(\mathrm{p})}$-dimensional pilot sequence vector of the kth UE, where $\|\boldsymbol{\varphi}_k\|^2 = 1$, and the corresponding received signal vector at the (l, n)-th antenna $\boldsymbol{y}_{l,n}^{(\mathrm{p})} \in \mathbb{C}^{\tau^{(\mathrm{p})}\times 1}$ can be written as [28]

$$\boldsymbol{y}_{l,n}^{(\mathrm{p})} = \sqrt{\rho^{(\mathrm{p})}\tau^{(\mathrm{p})}} \sum_{k=1}^{K} h_{l,n,k}\boldsymbol{\varphi}_k + \boldsymbol{z}_{l,n}^{(\mathrm{p})}. \quad (10)$$

Then, the MMSE channel estimate can be obtained as [28]

$$\hat{h}_{l,n,k} = \frac{\sqrt{\rho^{(\mathrm{p})}\tau^{(\mathrm{p})}}\beta_{l,k}}{\rho^{(\mathrm{p})}\tau^{(\mathrm{p})}\sum_{k'=1}^{K}\beta_{l,k'}\left|\boldsymbol{\varphi}_k^{\mathrm{H}}\boldsymbol{\varphi}_{k'}\right|^2 + 1} \boldsymbol{\varphi}_k^{\mathrm{H}}\boldsymbol{y}_{l,n}^{(\mathrm{p})}. \quad (11)$$

III. PERFORMANCE METRIC

This paper evaluates the performance of SE and EE from an antenna distribution point of view for each combining/precoding scheme and TPC algorithm. They will be expressed by using a general form of combining/precoding vectors.

A. UPLINK COMBINING SCHEMES

Uplink combining vectors of MRC and MMSE are given as follows by using the channel estimate obtained in (11):

$$\boldsymbol{v}_k = \begin{cases} \hat{\boldsymbol{h}}_k & (\mathrm{MRC}) \\ \rho^{(\mathrm{u})}q_k\left(\sum_{k'=1}^{K}\rho^{(\mathrm{u})}q_{k'}\left(\hat{\boldsymbol{h}}_{k'}\hat{\boldsymbol{h}}_{k'}^{\mathrm{H}} + \boldsymbol{C}_{k'}\right) + \boldsymbol{I}_{LN}\right)^{-1}\hat{\boldsymbol{h}}_k & (\mathrm{MMSE}), \end{cases} \quad (12)$$

where $\hat{\boldsymbol{h}}_k = [\hat{h}_{1,1,k}, \ldots, \hat{h}_{1,N,k}, \hat{h}_{2,1,k}, \ldots, \hat{h}_{L,N,k}]^{\mathrm{T}} \in \mathbb{C}^{LN\times 1}$ is the channel estimation vector whose elements are $\hat{h}_{l,n,k}$. $\boldsymbol{C}_{k'} = \tilde{\boldsymbol{h}}_{k'}\tilde{\boldsymbol{h}}_{k'}^{\mathrm{H}}$, and $\tilde{\boldsymbol{h}}_k$ is the channel estimation error and given by $\tilde{\boldsymbol{h}}_k = \boldsymbol{h}_k - \hat{\boldsymbol{h}}_k$. ZF is also one of the commonly used combiners, and can be obtained by omitting $\boldsymbol{C}_{k'}$ from MMSE combiner.

B. DOWNLINK PRECODING SCHEMES

In this paper, we use time division duplex. Due to channel reciprocity, the downlink precoding vector can be written as a re-normalized version of the uplink combining vector $\boldsymbol{v}_k$ of the corresponding weighting scheme (MRC or MMSE) as presented in (12):

$$\boldsymbol{w}_k = \sqrt{\rho^{(\mathrm{d})}\eta_k}\frac{\boldsymbol{v}_k}{\sqrt{\|\boldsymbol{v}_k\|^2}}, \quad (13)$$

where $\rho^{(\mathrm{d})}$ is the downlink transmit SNR. η_k is the transmit power coefficient allocated to the signals sent to the kth UE, which is in the range between 0 and 1, i.e., all APs use the same coefficient η_k for the kth UE.

C. SE

Based on [3], the uplink signal-to-interference-plus-noise ratio (SINR) of the kth UE at the receiver after the combining is given by

$$\mathrm{SINR}_k^{(\mathrm{u})} = \frac{\rho^{(\mathrm{u})}q_k\left|\boldsymbol{v}_k^{\mathrm{H}}\boldsymbol{h}_k\right|^2}{\sum_{k'\neq k}^{K}\rho^{(\mathrm{u})}q_{k'}\left|\boldsymbol{v}_k^{\mathrm{H}}\boldsymbol{h}_{k'}\right|^2 + \|\boldsymbol{v}_k\|^2}. \quad (14)$$

Similarly, the downlink SINR is given by

$$\mathrm{SINR}_k^{(\mathrm{d})} = \frac{\left|\boldsymbol{h}_k^{\mathrm{H}}\boldsymbol{w}_k\right|^2}{\sum_{k'\neq k}^{K}\left|\boldsymbol{h}_k^{\mathrm{H}}\boldsymbol{w}_{k'}\right|^2 + 1}. \quad (15)$$

Under the assumptions about the channel in Section II, and assuming transmission with capacity-achieving codes, the SE is obtained as follows by using the uplink or downlink SINR:

$$S_k = \log_2(1 + \mathrm{SINR}_k). \tag{16}$$

The SEs enter the objective of the max-min SE, the max-sum SE, and the max-min EE algorithms explained in the following section.

D. EE

Based on the generic approach of [29], we introduce a total power consumption model as follows:

$$P_{\mathrm{total}} = \bar{P}\sum_{k=1}^{K} q_k + KP_{\mathrm{U}} + L\left(P_{\mathrm{fix,AP}} + P_{\mathrm{bh,AP}}\right) + LN\left(P_{\mathrm{fix,ant}} + P_{\mathrm{bh,ant}}\right), \tag{17}$$

where $\bar{P}$ is the maximum transmit power, and P_{U} is the necessary power to run circuit components at each UE. The subscripts "fix," "bh," "AP," and "ant" denote fixed and backhaul power consumption as well as power consumption related each AP and antenna, respectively. In this paper, we assume that the baseline energy consumption of an AP is independent of the number of antenna elements.

In addition, P_{bh} of an AP or an antenna is given as follows by using the corresponding maximum power consumption P_{bt} for processing and backhauling the signal from each antenna elements:

$$P_{\mathrm{bh}} = P_{\mathrm{bt}}\frac{R_{\mathrm{bh}}}{C_{\mathrm{bh}}}, \tag{18}$$

where R_{bh} and C_{bh} are the actual and maximum backhaul rate, respectively.

More realistic models for power consumption can be considered but increase the complexity. Thus, we use this simplified power consumption model in this paper because the components appearing in (17) account for the majority of power consumption, and also because this model is commonly used in other papers in the literature [30], [31], [32].

When we focus on the power consumed only at the UE side, the power consumption is given by omitting AP-side components and expressed as

$$P_k = \bar{P}q_k + P_{\mathrm{U}}. \tag{19}$$

Therefore, the total (whole network) EE is given by

$$E_{\mathrm{total}} = \frac{\mathrm{Bandwidth}\cdot\sum_{k=1}^{K} w_k^{(\mathrm{b})} S_k}{P_{\mathrm{total}}}, \tag{20}$$

where $w_k^{(\mathrm{b})}$ is the weight for each UE. The weight can be chosen arbitrarily depending on the application and target, e.g., if the goal is to maximize the minimum lifetime of UE, the weight can be chosen proportional to the remaining battery charge.

Finally, EE of the kth UE is given by

$$E_k = \frac{\mathrm{Bandwidth}\cdot w_k^{(\mathrm{b})} S_k}{P_k}. \tag{21}$$

EE will be used as an objective of the max-min EE algorithm explained in detail in the following section.

IV. TPC ALGORITHMS

TPC is commonly used in practical cellular systems to reduce interference and improve the performance. The performance of each TPC algorithm depends on the antenna distribution. In this section, we introduce several TPC algorithms used for performance comparison.

A. MAX-POWER ALGORITHM

In the max-power algorithm, all UEs transmit signals with the maximum allowed power. For example, in the uplink, power control coefficients $q_k = 1$ for all UEs. One of the benefit of this algorithm is that it does not require any complicated calculation to obtain coefficient values. This is not strictly a TPC algorithm, but we investigate it to obtain a performance baseline against which to compare other TPC algorithms. With this algorithm, SE and EE per UE of each antenna distribution have the same tendency, i.e., the higher SE is, the higher EE is, because the denominator of (21) is constant with respect to UE power consumption.

B. MAX-MIN SE ALGORITHM

The max-min SE algorithm is one of the most commonly used TPC algorithms in CF-mMIMO papers. It aims to maximize the minimum SE among all UEs [2].

The maximization problem can be written as

$$\begin{aligned} &\mathrm{maximize}_{\{q_k\}} \ \min_{k=1,\ldots,K} S_k \\ &\text{subject to} \ \ 0 \le q_k \le 1, k = 1,\ldots,K. \end{aligned} \tag{22}$$

Since the logarithmic function in (16) increases monotonically as the SINR becomes larger, the problem (22) can be reformulated as follows:

$$\begin{aligned} &\mathrm{maximize}_{\{q_k\},t} \ \ t \\ &\text{subject to} \ \ t \le \mathrm{SINR}_k, k = 1,\ldots,K, \\ &\qquad\qquad 0 \le q_k \le 1, k = 1,\ldots,K. \end{aligned} \tag{23}$$

As described in [33], the problem (23) can be reformulated into a geometric programming (GP), and the proof is shown in Appendix A. Therefore, the objective function and constraints of the problem (23) are monomial and posynomial functions in terms of power coefficients. Since the problem (23) is a standard GP, it can be solved by convex optimization software, e.g., CVX for MATLAB [34], [35].

C. MAX-SUM SE ALGORITHM

The max-sum SE algorithm aims to maximize the total SE of all UEs, and the problem can be written as [36]

$$\begin{aligned} &\mathrm{maximize}_{\{q_k\}} \ \sum_{k=1}^{K} S_k \\ &\text{subject to} \ \ 0 \le q_k \le 1, k = 1,\ldots,K. \end{aligned} \tag{24}$$

The problem (24) can be rewritten as

$$\begin{aligned} \text{maximize}_{\{q_k,t_k\}} \quad & \prod_{k=1}^{K} t_k \\ \text{subject to} \quad & t_k \le 1 + \text{SINR}_k, k = 1, \ldots, K, \\ & 0 \le q_k \le 1, k = 1, \ldots, K. \end{aligned} \tag{25}$$

As described in [36], the problem (25) can be reformulated into GP, and the proof is shown in Appendix B.

Note that transmit power of some UEs might be set to extremely small value if it helps to increase the sum SE.

D. MAX-MIN EE ALGORITHM

Operating networks in an energy-efficient way is a common target worldwide. Inspired by the formulation of the max-min SE algorithm, the max-min EE algorithm aims to maximize the minimum EE while meeting the required minimum SE, and its optimization problem can be written as

$$\begin{aligned} \text{maximize}_{\{q_k\}} \quad & \min_{k=1,\ldots,K} E_k \\ \text{subject to} \quad & S_k \ge S_k^{(\text{r})}, k = 1, \ldots, K, \\ & 0 \le q_k \le 1, k = 1, \ldots, K, \end{aligned} \tag{26}$$

where $S_k^{(\text{r})}$ is the required minimum SE for the kth UE to ensure a certain level of quality of service. The value of $S_k^{(\text{r})}$ depends on the use cases of each UE. In this paper, for simplicity, we assume that $S_k^{(\text{r})}$ is the common value among all UEs, and denote it as $S^{(\text{r})}$ henceforth.

According to the definition of E_k in (21), the problem (26) can be reformulated as follows:

$$\begin{aligned} \text{maximize}_{\{q_k\}} \quad & \min_{k=1,\ldots,K} \frac{\text{Bandwidth} \cdot w_k^{(\text{b})} S_k}{\bar{P} q_k + P_{\text{U}}} \\ \text{subject to} \quad & S_k \ge S^{(\text{r})}, k = 1, \ldots, K, \\ & 0 \le q_k \le 1, k = 1, \ldots, K. \end{aligned} \tag{27}$$

To make the problem easier to handle, replace q_k in the denominator with an auxiliary variable ν:

$$\begin{aligned} \text{maximize}_{\{q_k\},\nu} \quad & \min_{k=1,\ldots,K} \frac{\text{Bandwidth} \cdot w_k^{(\text{b})} S_k}{\bar{P} \nu + P_{\text{U}}} \\ \text{subject to} \quad & S_k \ge S^{(\text{r})}, k = 1, \ldots, K, \\ & 0 \le q_k \le 1, k = 1, \ldots, K, \\ & q_k \le \nu, k = 1, \ldots, K, \\ & \nu^* \le \nu \le 1, \end{aligned} \tag{28}$$

where ν^* is the slack variable and given as the maximum q_k obtained by solving the following optimization problem:

$$\begin{aligned} \text{maximize}_{\{q_k\}} \quad & \min_{k=1,\ldots,K} q_k \\ \text{subject to} \quad & S_k \ge S^{(\text{r})}, k = 1, \ldots, K, \\ & 0 \le q_k \le 1, k = 1, \ldots, K. \end{aligned} \tag{29}$$

TABLE 1. Basic parameter specifications [39].

Total number of antennas (LN)	256
Number of UEs (K)	8
Area size	1 km × 1 km
Number of UE drops	500
Carrier frequency	3.5 GHz
Bandwidth	20 MHz
Noise power	−92 dBm
Fading	Rician
Rician K-factor in dB	$13 - 0.03 \cdot$ Distance
Reference distance (d_0)	1 m
Median channel gain at d_0 (g_0)	−43.3 dB
Path loss exponent (γ)	2
Azimuth angular standard deviation (σ_ϕ)	20°
Uplink data power ($\bar{P}$)	0.2 W
UE circuit power consumption (P_{U})	0.1 W
Shadowing standard deviation (σ_{s})	8 dB

It can be proved that the optimal solutions of the problems (26) and (28) are equal [37]. Therefore, ν^* is given by

$$\nu^* = \frac{\sum_{k=1}^{K} q_k^+}{K}, \tag{30}$$

where q_k^+ is the optimal solution of the problem (29).

It is noted that the objective function of the problem (28) increases monotonically when ν is in the range of $\nu^* \le \nu \le \nu^{\text{opt}}$, and decreases monotonically in the range of $\nu^{\text{opt}} \le \nu \le 1$. Therefore, ν^{opt} can be obtained by using a simple linear search algorithm, e.g., the hill-climbing algorithm [37].

Then, the problem (28) can be solved as follows:

1) Find the optimal value of ν to maximize the minimum EE using a linear search algorithm.
2) Optimize q_k to maximize the minimum EE while ensuring the required minimum SE.

V. NUMERICAL EVALUATION

In this section, we present evaluations of SE and EE for semi-distributed systems as well as the fully-distributed and concentrated systems, based on Monte Carlo simulations. Table 1 shows the basic parameters of numerical simulations. The values listed on the table will be applied unless other values are mentioned specifically. APs and UEs are distributed following a uniform distribution, i.e., a binomial point process. In addition, we assume that the pilot signal of every UE is orthogonal with each other, i.e., there is no pilot contamination. Pilot contamination degrades the accuracy of channel estimation, which makes performance worse. The Rician K-factor is a function of the distance between an AP and a UE, following the model of the 3GPP channel model [38]. The required minimum SE $S^{(\text{r})}$ will be mentioned with each result. For simplicity, we set weight $w_k^{(\text{b})}$ to 1 for all UEs.

In this paper, we fix the total number of antennas (LN). Therefore, the number of antennas on each AP (N) is determined based on the number of APs (L).

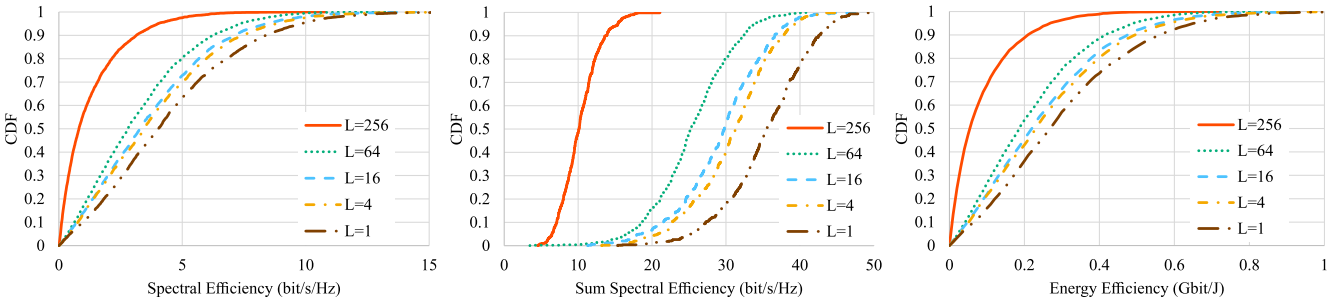

(a) SE per UE (b) Sum SE (c) EE per UE

FIGURE 2. The SE, sum SE, and EE performance for MRC without TPC. The performance is evaluated with various values of the number of APs (L) from fully-distributed ($L = 256$) to concentrated ($L = 1$).

As we assume that the (l, n)-th antenna is placed on the lth AP following the notation of Section II, the large-scale fading is given as follows, based on [40], [41]:

$$\beta_{l,k} = g_0 - 10\gamma \log_{10}\left(\frac{d_{l,k}}{d_0}\right) + \frac{\sigma_\omega^2}{\sqrt{2}}\left(\omega_l^{\mathrm{AP}} + \omega_k^{\mathrm{UE}}\right), \quad (31)$$

where $d_{l,k}$ is the distance between the lth AP and the kth UE. ω_l^{AP} and ω_k^{UE} are normalized shadow fading of the lth AP and the kth UE, respectively, and σ_ω^2 is its variance. Although shadowing is related to the link, and not separately to the AP and UE, splitting the total link shadowing into two contributions following [40], [41] is expected to (approximately) consider the shadowing correlation between different UEs and APs, respectively.

In addition, we assume that each AP has a uniform linear antenna array (ULA), and an element $p_{l,n,k}^{(\mathrm{LoS})}$ of a vector $\boldsymbol{p}_{l,k}^{(\mathrm{LoS})}$ is given as

$$p_{l,n,k}^{(\mathrm{LoS})} = \exp\left(2\pi \mathrm{j} d_{\mathrm{a}}(n-1)\sin\left(\phi_{l,k}\right)\sin\left(\theta_{l,k}\right)\right), \quad (32)$$

where d_{a} is the distance between adjacent antennas within an AP, $\phi_{l,k}$ and $\theta_{l,k}$ denotes the azimuth and the elevation angles between the lth AP and the kth UE, respectively. Similarly, following a model presented in [42], an element $r_{n_1,n_2}^{(\mathrm{NLoS},l,k)}$ of a matrix $\boldsymbol{R}_{l,k}$ is defined between two adjacent antennas and given by (33), shown at the bottom of the page.

In this paper, the hill-climbing algorithm is applied to optimize ν. The initial value is set as $\nu^{\mathrm{init}} = \nu^*$. The step size for each iteration is set to 0.1, and ν approaches 1. If the obtained minimum EE is smaller than that of the previous point, the step size will be divided by 3 and the sign will be inverted, i.e., the point will turn back with a smaller step. The iteration will end if the step size becomes smaller than 10^{-4}.

This section is organized as follows: First, we analyze uplink SE and EE performance without TPC for MRC and MMSE. Then, we focus on the performance of uplink MMSE with TPC, uplink MRC with TPC, and downlink MMSE with/without TPC. Note that all simulations in this section assume channel estimation error, i.e., non-ideal knowledge of CSI.

A. UPLINK

1) SE AND EE PERFORMANCE WITHOUT TPC

In this section, we investigate the SE and EE performance difference between MRC and MMSE with the max-power algorithm, i.e., no TPC is applied. These results are the basis of performance comparison in the following sections. As mentioned in Section IV-A, SE and EE show similar performance in terms of antenna distribution because the power consumption of each UE is the same.

Although simulation results include channel estimation errors, *if* we assume that the channel is estimated perfectly, the SINR (14) can be reformulated as follows:

$$\mathrm{SINR}_k = \frac{\rho \boldsymbol{v}_k^{\mathrm{H}} \boldsymbol{h}_k \boldsymbol{h}_k^{\mathrm{H}} \boldsymbol{v}_k}{\sum_{k' \neq k}^{K} \rho \boldsymbol{v}_k^{\mathrm{H}} \boldsymbol{h}_{k'} \boldsymbol{h}_{k'}^{\mathrm{H}} \boldsymbol{v}_k + \boldsymbol{v}_k^{\mathrm{H}} \boldsymbol{v}_k}. \quad (34)$$

Note that we can omit q_k because $q_k = 1$ for the max-power algorithm. By applying the Rayleigh quotient [42], the maximum SINR is expressed by

$$\mathrm{SINR}_k^{(\max)} = \boldsymbol{h}_k^{\mathrm{H}} \boldsymbol{v}_k. \quad (35)$$

1) MRC: Fig. 2 shows the performance of SE, sum SE, and EE for MRC, respectively. As can be seen in Fig. 2(a), the concentrated deployment has the best performance. This is because the phenomena of channel hardening and favorable propagation becomes stronger when larger numbers of antennas gather at one spot [3]. Another finding is that the starting point of CDF curves for all antenna distributions are extremely close to 0. The reason for this is that MRC cannot mitigate interference caused by other UEs with the maximum transmit power.

$$r_{n_1,n_2}^{(\mathrm{NLoS},l,k)} = \int_{-\infty}^{\infty} \exp\left(2\pi \mathrm{j} d_{\mathrm{a}}(n_1 - n_2)\sin\left(\phi_{l,k} + \delta_{\mathrm{a}}\right)\sin\left(\theta_{l,k}\right)\right) \frac{1}{\sqrt{2\pi}\sigma_\phi} \exp\left(-\frac{\delta_{\mathrm{a}}^2}{2\sigma_\phi^2}\right) \mathrm{d}\delta_{\mathrm{a}} \quad (33)$$

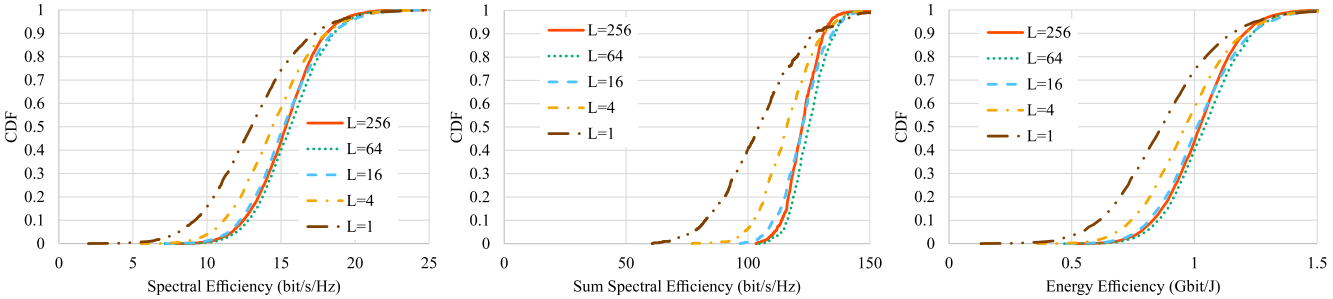

(a) SE per UE (b) Sum SE (c) EE per UE

FIGURE 3. The SE, sum SE, and EE performance for MMSE without TPC. The performance is evaluated with various values of the number of APs (L) from fully-distributed ($L = 256$) to concentrated ($L = 1$).

In Fig. 2(b), the gap between each antenna distribution becomes narrower as the number of APs decreases, however, the gap between $L = 4$ and $L = 1$ is wider than that of $L = 16$ and $L = 4$. The reason is the same as for the SE performance, i.e., the channel hardening phenomenon is very strong for $L = 1$ because all AP antennas are gathered at one spot. And Fig. 2(c) shows the same shape as in Fig. 2(a) since the transmit powers of all UEs are the same, which is included in the denominator of EE.

2) MMSE: Fig. 3 shows the performance of SE, sum SE, and EE for MMSE, respectively. Compared to Fig. 2, the overall performance of SE, sum SE and EE for MMSE is better than that for MRC. This is because the MMSE combiner can mitigate the interference from surrounding UEs. While it has been established that for concentrated MIMO, in the limit of very large number of antenna elements, MRC can suppress interference [43], LN in our investigations (up to 256) is smaller than the regime in which this happens; furthermore, in the distributed case, the convergence of MRC is even slower.

For all three performance measures, $L = 64$ outperforms $L = 256$. Furthermore, $L = 16$ also shows similar performance as $L = 64$ and $L = 256$, which means that the number of APs can be reduced by 75% while keeping the UE performance essentially the same. This result is also helpful for network operators because they can cut down the cost of system deployment. Unlike the MRC case, $L = 1$ shows the worst performance. This is because the distance between an AP and a UE becomes longer as the number of APs decreases, and the total received power also decreases.

The relationship between the performance and antenna distributions for MMSE is analyzed in Appendix C.

2) MMSE WITH TPC

In this section, the performance for MMSE with applying TPC is evaluated. Fig. 4 shows the 5- and 50-percentile SE/sum SE performance with various number of AP locations. Note that, in the figure, the performance of 5- and 50-percentile SE is obtained by applying the max-min SE algorithm, and the performance of 5- and 50-percentile sum SE is obtained by applying the max-sum SE algorithm.

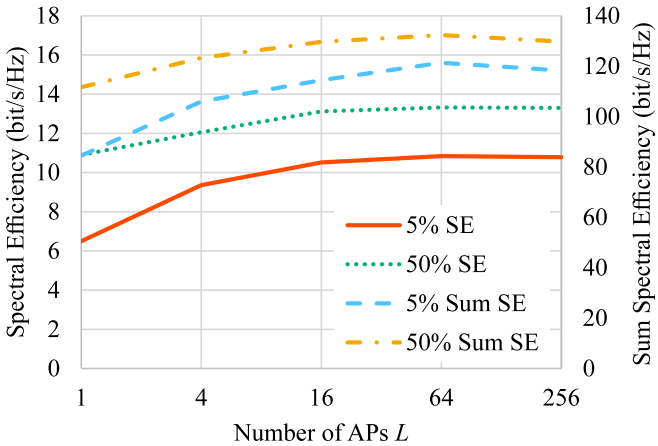

FIGURE 4. The SE performances for MMSE with the max-min SE algorithm, and the sum SE performance with the max-sum SE algorithm. The corresponding vertical axis of each performance is on the left and the right, respectively.

As can be seen, all performances improve as the number of APs becomes larger, and converge in the range between $L = 16$ and $L = 256$. Especially, there are maxima at $L = 64$ for every case. This means that the semi-distributed deployments have superiority for both average UE performance and outage performance.

Fig. 5 shows the EE performance with the max-min EE algorithm. The minimum SE for all UEs is 5 bit/s/Hz in Fig. 5(a) and 15 bit/s/Hz in Fig. 5(b). As can be seen in Fig. 3(a), most of UEs can achieve 5 bit/s/Hz, therefore, the CDF curves are smooth. In addition, compared to Fig. 3(c), the range of EE becomes wider. This is because the transmit power of most UEs is reduced to meet the minimum required SE, which means the interference to surrounding UEs is also reduced. On the other hand, nearly half of UEs cannot achieve 15 bit/s/Hz, therefore the slope of CDF curves decreases at 1 Gbit/J. In addition, for the same reason, the gap between $L = 256$ and $L = 1$ becomes narrower at lower CDF.

Fig. 5(c) shows the EE performance of minimum SE 5 bit/s/Hz with random $w_k^{(b)}$, each of which follows the uniform distribution in the range of $(0, 1)$. Note that the result can vary depending actual realization of $w_k^{(b)}$. Compared

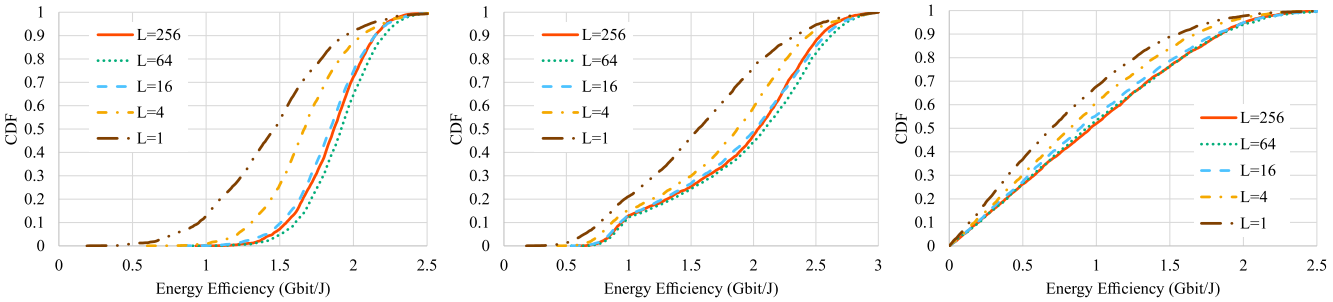

(a) Minimum SE: 5 bit/s/Hz (b) Minimum SE: 15 bit/s/Hz (c) Minimum SE: 5 bit/s/Hz, Random $w_k^{(b)}$

FIGURE 5. The EE performance for MMSE of each UE with different minimum SE, i.e., 5 bit/s/Hz and 15 bit/s/Hz. The performance with random $w_k^{(b)}$ with minimum SE 5 bit/s/Hz is also investigated. The performance is evaluated with various values of the number of APs (L) from fully-distributed ($L = 256$) to concentrated ($L = 1$).

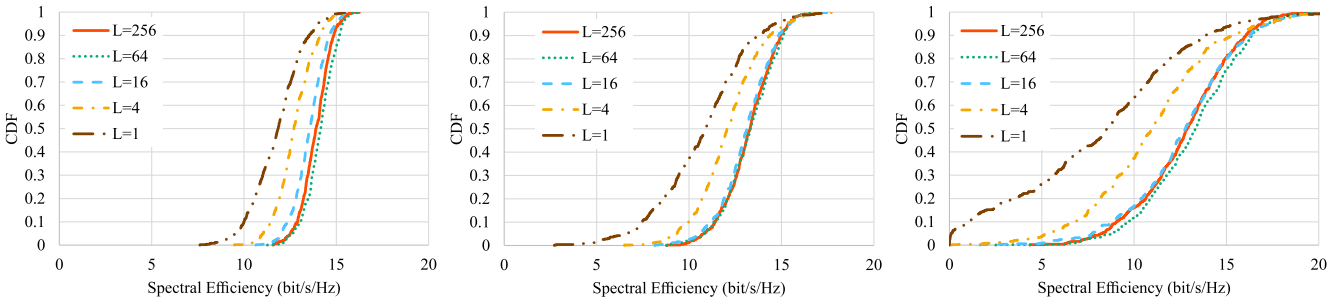

(a) $\sigma_s = 4$ dB (b) $\sigma_s = 8$ dB (c) $\sigma_s = 16$ dB

FIGURE 6. The SE performance for MMSE with various values of shadowing standard deviation. Note that the shadowing effects become stronger as the standard deviation increases. The performance is evaluated with various values of the number of APs (L) from fully-distributed ($L = 256$) to concentrated ($L = 1$).

TABLE 2. The minimum SEs (bit/s/Hz) and EE (Gbit/J) for MMSE ($S^{(r)} = 5$ bit/s/Hz for EE performance).

		$L = 256$	$L = 64$	$L = 16$	$L = 4$	$L = 1$
SE	No TPC	7.86	7.16	7.25	5.54	1.99
	Max-min SE	8.79	8.13	8.16	6.51	2.72
Sum SE	No TPC	103	105	96.9	77.1	60.8
	Max-sum SE	111	112	104	84.3	67.2
EE	No TPC	0.524	0.478	0.483	0.369	0.133
	Max-min EE	0.937	0.837	0.841	0.609	0.193

to Fig. 5(a), performance of all antenna distribution is degraded. This is because $w_k^{(b)}$ of some UEs, especially which suffer from bad channel conditions, is degraded drastically. It will be future work to investigate the performance by setting $w_k^{(b)}$ according to each UE's environment.

Finally, Table 2 shows the minimum SE, sum SE, and EE obtained by applying corresponding TPC algorithms compared to max-power algorithm, i.e., without TPC. Each TPC algorithm works to achieve the goal shown in its name. For example, max-min SE tries to maximize the minimum SE and has no responsibility to maximize sum-SE or the minimum EE. The same can be said for the max-sum SE and the max-min EE algorithms. Therefore, for instance, comparison of sum-SE performance between the max-sum SE algorithm and the max-min SE algorithm does not provide significant insights. This is why we show the performance comparison between each TPC algorithm and "no TPC." Note that $S^{(r)} = 5$ bit/s/Hz for the max-min EE algorithm. The minimum SE improves by 15% on average and up to 37% for $L = 1$. The minimum sum SE improves by about 8%. And the minimum EE improves by 75% on average. As can be seen, the growth rate of EE is the highest among all three performance metrics. EE is one of the important key indicators for B5G systems, and the max-min EE algorithm will be useful method to improve UE performance.

1) Shadowing effects on SE: In this section, we investigate the effects of shadowing on SE for MMSE. Shadowing standard deviations σ_s of 4, 8, and 16 dB are evaluated.

As can be seen in Fig. 6(c), the performance for $L = 1$ degrades dramatically compared to other deployments, due to an absence of macro-diversity. In other words, gathering all antennas at one spot causes performance degradation to all channels when this spot is in a shadowing dip. On the other hand, if antennas are distributed at different spots, some channels suffer from severe shadowing dips while others are in shadowing peaks, leading to an improvement in at least some cases. The shadowing does not affect the superiority/inferiority of each antenna distribution for MMSE compared to MRC which is investigated in the following section.

3) MRC WITH TPC

In this section, the performance for MRC with applying TPC is evaluated. Fig. 7 shows the 5- and 50-percentile SE/sum SE performance with various number of APs. Note that, in

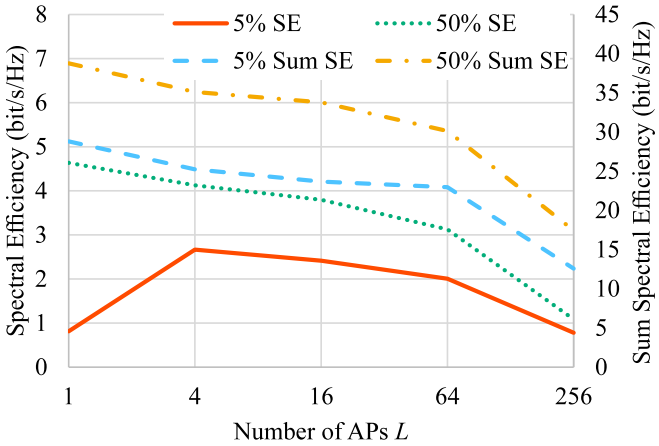

FIGURE 7. The SE performances for MRC with the max-min SE algorithm, and the sum SE performance with the max-sum SE algorithm is shown. The corresponding vertical axis of each performance is on the left and the right, respectively.

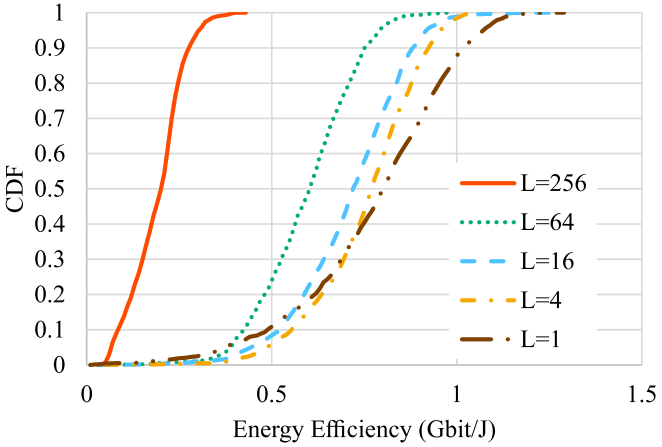

FIGURE 8. The EE performance for MRC with $S^{(r)} = 1$ bit/s/Hz. The performance is evaluated with various values of the number of APs (L) from fully-distributed ($L = 256$) to concentrated ($L = 1$).

the figure, the performance of 5- and 50-percentile SE is obtained by applying the max-min SE algorithm, and the performance of 5- and 50-percentile sum SE is obtained by applying the max-sum SE algorithm.

As can be seen, the performance is degraded as the number of APs becomes larger, except for 5-percentile SE. This is because the channel hardening phenomenon becomes stronger. The fully-distributed deployment has the worst performance in all cases. On the other hand, concentrated deployment suffers from shadowing effects more drastically than other antenna distributions because all AP antennas are gathered at one spot and are affected by the same shadowing effects. On average (i.e., for the 50-percentile), concentrated arrays enable good suppression of interference because (for MRC) the normalized inner product of two random Gaussian vectors converges more quickly to zero when the statistics of those two vectors are identical. However, the UEs that have low performance (i.e., accounting for the bottom part of the CDF) are the ones suffering from deep shadowing. Since a concentrated array provides only micro-diversity, but no macro-diversity, distributed arrays perform better. This is the reason why semi-distributed deployments are superior to the concentrated deployment for 5-percentile SE. The effect of shadowing on SE is further investigated in the following section.

Fig. 8 shows the EE performance for MRC with $S^{(r)} = 1$ bit/s/Hz. The value is selected based on the result shown in Fig. 2(a), where almost 90% of the UEs can achieve it. It is important to select an appropriate value of SE because the max-min EE algorithm assumes each UE can achieve the minimum required SE. However, for MRC, the minimum SE without TPC is almost 0, therefore we have no choice but to select 1 for the minimum required SE. Compared to Fig. 2(c), the performance is completely different. This means that, by applying the max-min EE algorithm, outage performance can be improved even though there is no interference mitigation in MRC itself.

TABLE 3. The minimum SEs (bit/s/Hz) and EE (Mbit/J) for MRC ($S^{(r)} = 1$ bit/s/Hz for EE performance).

		$L = 256$	$L = 64$	$L = 16$	$L = 4$	$L = 1$
SE	No TPC	0.00317	0.00480	0.00193	0.00464	0.000795
	Max-min SE	0.586	0.528	0.895	1.11	0.105
Sum SE	No TPC	4.50	3.48	11.3	13.2	15.3
	Max-sum SE	9.01	11.6	15.1	18.4	22.0
EE	No TPC	0.211	0.320	0.128	0.310	0.0530
	Max-min EE	112	157	264	338	179

Finally, Table 3 shows the minimum SE, sum SE, and EE obtained by applying corresponding TPC algorithms compared to the max-power algorithm, i.e., without TPC. Note that $S^{(r)} = 1$ bit/s/Hz for the max-min EE algorithm, and the unit for EE is Mbit/J. By applying the max-min SE algorithm, the SE performance improved by more than 100%. The remarkable phenomenon with the max-sum SE algorithm is that the transmit power of some UEs are set to 0. Since MRC cannot mitigate interference, it might be good to "mute" some UEs to increase the total SE. This tendency is more remarkable as the number of APs is larger. When we need to keep SE of each UE at a certain level while optimizing the sum SE, a possible solution is to set the required minimum SE as shown in the max-min EE algorithm. EE performance with the max-min EE algorithm improves significantly; this is because almost all UEs can achieve the required minimum SE as mentioned in the previous paragraph. This leads the transmit power reduction and improves the EE. The improvement varies depending on the required minimum SE.

1) Shadowing effects on SE: On the other hand, shadowing effects prominently impact the absolute performance of MRC. Thus, in this section, we investigate the effects of shadowing on SE for MRC. The shadowing standard deviation σ_s of 4, 8, and 16 dB are evaluated.

As can be seen on Fig. 9(c), the performance for $L = 1$ degrades dramatically compared to other deployments. This

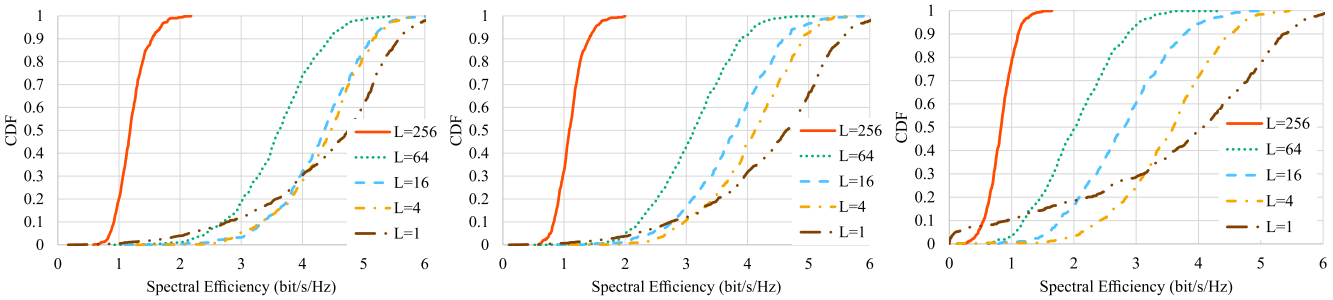

(a) $\sigma_s = 4$ dB (b) $\sigma_s = 8$ dB (c) $\sigma_s = 16$ dB

FIGURE 9. The SE performance for MRC with various values of shadowing standard deviation. Note that the shadowing effects become stronger as the standard deviation increases. The performance is evaluated with various values of the number of APs (L) from fully-distributed ($L = 256$) to concentrated ($L = 1$).

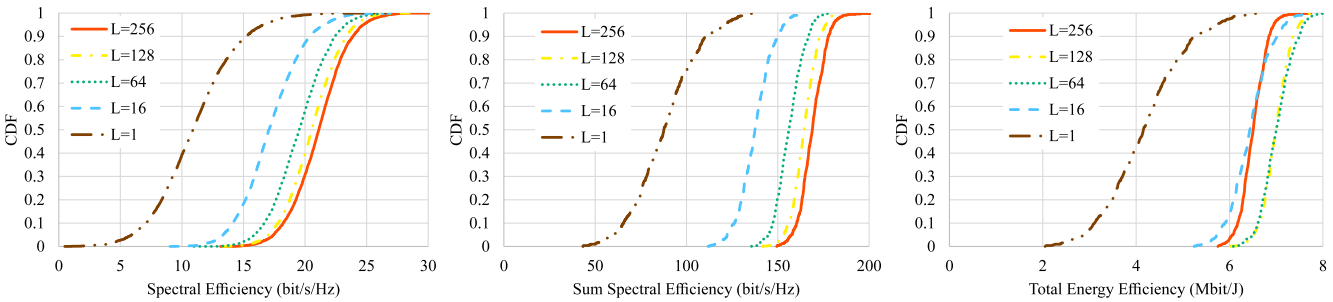

(a) SE per UE (b) Sum SE (c) EE per UE

FIGURE 10. The downlink SE, sum SE, and EE performance for MMSE without TPC. The performance is evaluated with various values of the number of APs (L) from fully-distributed ($L = 256$) to concentrated ($L = 1$).

is because gathering all antennas at one spot causes performance degradation to all channels when shadowing realization is worse. On the other hand, if antennas are distributed at different spots, some channels suffer from severe shadowing dips while others are in shadowing peaks, leading to an improvement in at least some cases. Finally, when we focus on the outage probability, the semi-distribution shows the best performance. This indicates that semi-distribution is robust with respect to various kinds of channel environments especially for the UEs which suffer from bad channel condition.

From the results on Fig. 9(a), the performance of $L = 1$ does not change so much compared to Fig. 9(b). On the other hand, semi-distributed deployments improve their performance. This is because semi-distribution have more realizations of shadowing than the concentrated deployment, and which not only averages out channel variations, but even increases the chance of "opportunistic" shadowing peaks that provide improved SNR. In summary, at the phase of deploying CF-mMIMO systems in a practical environment, semi-distributed deployments are robust to account for the shadowing effects, and reduce the cost of deploying hardware and cables.

B. DOWNLINK

1) SE AND EE PERFORMANCE WITHOUT TPC

In this section, we investigate the downlink SE and EE performance of MMSE with the max-power algorithm, i.e., no TPC is applied. These results are the basis of the performance comparison in the following sections.

Fig. 10 shows the downlink performance of SE, sum SE, and total EE for MMSE, respectively. Note that SE is computed according to Shannon's formula, though actually realizing values above 10 bit/s/Hz with practical transceivers might be challenging. In addition, for the downlink, the total EE is investigated instead of EE per UE. This is because power is mainly consumed in APs, not UEs. Compared to Fig. 3, the performance gap between $L = 256$ and $L = 1$ becomes wider. One of the reason is that the more APs are near an UE, the higher power the UE can receive. Although $L = 256$ has the best performance of SE and sum SE, $L = 128$ has similar performance. This result indicates that we can reduce the number of APs by half while keeping almost the same performance as the fully-distributed deployment.

On the other hand, $L = 128$ and $L = 64$ show better total EE performance than $L = 256$. This is because total EE performance is obtained with a trade-off between sum SE and total power consumption. In this paper, we assume that the power consumption ratio associated with an antenna to that associated with an AP as a whole is 9 to 1.[5] The fact that $L = 128$ and $L = 64$ consume less power while

5. This is based on that the signal processing effort for an antenna signal consumes more power than the "overall" AP signal processing.

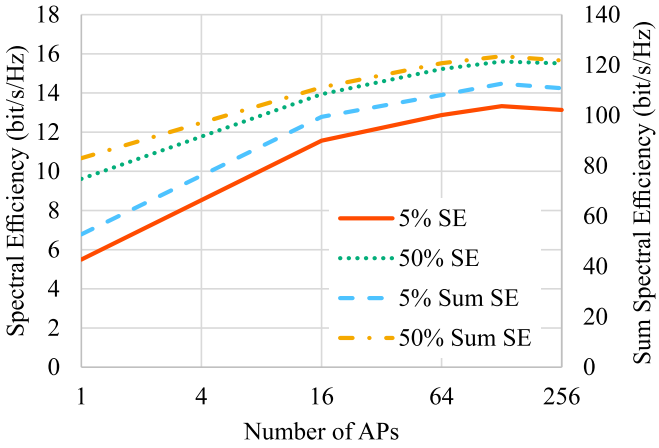

FIGURE 11. The downlink SE performances for MMSE with the max-min SE algorithm, and the sum SE performance with the max-sum SE algorithm. The corresponding vertical axis of each performance is on the left and the right, respectively.

suffering only a small degradation of SE performance results in better total EE performance.

2) MMSE WITH TPC

In this section, the downlink performance for MMSE with TPC is evaluated. Fig. 11 shows the 5- and 50-percentile SE/sum SE performance with various numbers of AP locations. Note that, in the figure, the performance of 5- and 50-percentile SE is obtained by applying the max-min SE algorithm, and the performance of 5- and 50-percentile sum SE is obtained by applying the max-sum SE algorithm.

As can be seen, similar to Fig. 4, all performances improve as the number of APs becomes larger in the range between $L = 1$ and $L = 128$. There are maxima at $L = 128$ for every case and the performance becomes worse for $L = 256$. This means that the semi-distributed deployments have superiority for both average UE performance and outage performance.

VI. CONCLUSION

In this paper, we investigated the SE and EE performance of CF-mMIMO systems in terms of antenna distributions. With various kinds of TPC algorithms and UE combining/precoding schemes, we clarified that we can obtain similar performance of SE and EE with a specific combining scheme regardless of TPC algorithms.

In uplink MRC, the concentrated deployment has the best average SE performance thanks to the channel hardening. When we focus on the performance improvements of UEs which suffer from severely bad environment, semi-distributed deployments outperform the concentrated deployment. This tendency is more remarkable when the effects of shadowing become stronger.

In uplink/downlink MMSE, the semi-distributed deployments have almost the same performance as the fully-distributed deployment, and we can reduce the number of APs to 1/4 for uplink and to 1/2 for downlink while keeping UE performance essentially the same.

APPENDIX A
POSYNOMIAL FORM OF SINR CONSTRAINT

First, the SINR constraint in (23) can be rewritten as a form of posynomial function as follows:

$$\frac{1}{q_k}\left(\sum_{k'\neq k}^{K} e_{k,k'}q_{k'} + \sum_{k'=1}^{K} f_{k,k'}q_{k'} + r_k\right) < \frac{1}{t}, \tag{36}$$

where

$$e_{k,k'} = \frac{\left(\sum_{l=1}^{L}\sum_{n=1}^{N}\mathbb{E}\left\{\left|\hat{h}_{l,n,k}\right|^2\right\}\frac{\beta_{l,k'}}{\beta_{l,k}}\right)^2\left|\boldsymbol{\varphi}_k^{\mathrm{H}}\boldsymbol{\varphi}_{k'}\right|^2}{\left(\sum_{l=1}^{L}\sum_{n=1}^{N}\mathbb{E}\left\{\left|\hat{h}_{l,n,k}\right|^2\right\}\right)^2}, \tag{37}$$

$$f_{k,k'} = \frac{\sum_{l=1}^{L}\sum_{n=1}^{N}\mathbb{E}\left\{\left|\hat{h}_{l,n,k}\right|^2\right\}\beta_{l,k'}}{\left(\sum_{l=1}^{L}\sum_{n=1}^{N}\mathbb{E}\left\{\left|\hat{h}_{l,n,k}\right|^2\right\}\right)^2}, \tag{38}$$

$$r_k = \frac{\sum_{l=1}^{L}\sum_{n=1}^{N}\mathbb{E}\left\{\left|\hat{h}_{l,n,k}\right|^2\right\}}{\rho\left(\sum_{l=1}^{L}\sum_{n=1}^{N}\mathbb{E}\left\{\left|\hat{h}_{l,n,k}\right|^2\right\}\right)^2}. \tag{39}$$

The left-hand side of (36) is a posynomial function.

APPENDIX B
HOW TO SOLVE THE PROBLEM (25)

First, we define a function as follows:

$$f(q_k) = 1 + \mathrm{SINR}_k. \tag{40}$$

For any polynomial $g(x) = m_i(x)$, where i is the index of iteration, it can be said for any α_i that

$$g(x) \geq \tilde{g}(x) = \prod_i \left(\frac{m_i(x)}{\alpha_i}\right)^{\alpha_i}. \tag{41}$$

As shown in (14), SINR is a fraction. Therefore, the SINR constraint in the problem (25) can be expressed as:

$$\frac{f_k(q_{k'})}{g_k(q_{k'})} \geq t_k. \tag{42}$$

By replacing $f_k(q_{k'})$ with a monomial $\tilde{f}_k(q_{k'})$, the SINR constraint can be converted as

$$\tilde{f}_k(q_{k'}) \geq t_k g_k(q_{k'}). \tag{43}$$

Finally, the problem (25) can be transformed into GP by repeating the conversion for all UEs.

APPENDIX C
PERFORMANCE AND ANTENNA DISTRIBUTION FOR MMSE

SINR for MMSE is given by

$$\mathrm{SINR}_k = \rho\boldsymbol{h}_k^{\mathrm{H}}\left(\sum_{k'=1}^{K}\rho\boldsymbol{h}_{k'}\boldsymbol{h}_{k'}^{\mathrm{H}} + \boldsymbol{I}_M\right)^{-1}\boldsymbol{h}_k. \tag{44}$$

Note that we can omit q_k because $q_k = 1$ for the max-power algorithm. In order to omit the variation of small-scale fading coefficients, the expectation operation over the small-scale fading is taken:

$$\mathbb{E}\{\mathrm{SINR}_k\} = \rho \boldsymbol{h}_k^{\mathrm{H}} \left(\sum_{k'=1}^{K} \rho \mathbb{E}\{\boldsymbol{h}_{k'} \boldsymbol{h}_{k'}^{\mathrm{H}}\} + \boldsymbol{I}_{LN} \right)^{-1} \boldsymbol{h}_k. \quad (45)$$

Here, the expectation of channel coefficients is given by a correlation matrix $\boldsymbol{R}_k^{(\mathrm{ch}) \in \mathbb{C}^{LN \times LN}}$ whose elements are in the range between 0 and 1. For example, when all antennas are distributed, $\boldsymbol{R}_k^{(\mathrm{ch})} = \boldsymbol{I}_{LN}$. On the other hand, when all the AP antennas are concentrated (conventional massive MIMO setup), $\boldsymbol{R}_k^{(\mathrm{ch})}$ is given as follows:

$$\boldsymbol{R}_k^{(\mathrm{ch})} = \begin{bmatrix} 1 & r_{12} & r_{13} & \cdots & r_{1M} \\ r_{21} & 1 & r_{23} & \cdots & r_{2M} \\ \vdots & \ddots & \ddots & \ddots & \vdots \\ \vdots & \ddots & \ddots & 1 & r_{(M-1)M} \\ r_{M1} & \cdots & \cdots & r_{M(M-1)} & 1 \end{bmatrix}, \quad (46)$$

where $0 < r < 1$, and the diagonal elements are 1.

When the antennas are semi-distributed, some elements are exactly 0 because antennas of different APs are uncorrelated. For instance, assuming that $N = 2$:

$$\boldsymbol{R}_k^{(\mathrm{ch})} = \begin{bmatrix} 1 & r_{12} & 0 & \cdots & 0 \\ r_{21} & 1 & 0 & \cdots & \vdots \\ 0 & \ddots & \ddots & \ddots & 0 \\ \vdots & \ddots & \ddots & 1 & r_{(M-1)M} \\ 0 & \cdots & 0 & r_{M(M-1)} & 1 \end{bmatrix}, \quad (47)$$

where 2×2 sub-matrices are placed diagonally, and other elements are 0. Note that the more antennas each AP has, the more non-zero elements the correlation matrix includes. Therefore, UE performance can be highly affected, i.e., it improves or degrades drastically by channel variations due to the concentrated antennas. On the other hand, when antennas are distributed, UE performance will be averaged. However, too small number of antennas may obtain lower desired received signal power compared to interference and noise power, which cause UE performance degradation. The total performance depends on the balance of channel correlation and interference suppression, and can be future work for investigation.

REFERENCES

[1] A. F. Molisch, *Wireless Communications: From Fundamentals to Beyond 5G*, 3rd ed. Hoboken, NJ, USA: Wiley, Dec. 2022.

[2] H. Q. Ngo, A. Ashikhmin, H. Yang, E. G. Larsson, and T. L. Marzetta, "Cell-free massive MIMO versus small cells," *IEEE Trans. Wireless Commun.*, vol. 16, no. 3, pp. 1834–1850, Mar. 2017.

[3] Ö. T. Demir, E. Björnson, and L. Sanguinetti, "Foundations of user-centric cell-free massive MIMO," *Found. Trends Signal Process.*, vol. 14, nos. 3–4, pp. 162–472, 2021. [Online]. Available: http://dx.doi.org/10.1561/2000000109

[4] H. Tataria, M. Shafi, A. F. Molisch, M. Dohler, H. Sjöland, and F. Tufvesson, "6G wireless systems: Vision, requirements, challenges, insights, and opportunities," *Proc. IEEE*, vol. 109, no. 7, pp. 1166–1199, Jul. 2021.

[5] N. Rajatheva *et al.*, "White paper on broadband connectivity in 6G: 6G research visions, no. 10," 6G Flagship, Univ. Oulu, Oulu, Finland, White Paper, Jun. 2020. [Online]. Available: http://jultika.oulu.fi/files/isbn9789526226798.pdf

[6] "Beyond 5G/6G, version 2.0.1," KDDI Corp. KDDI Res., Inc., Tokyo, Japan, White Paper, Oct. 2021. [Online]. Available: https://www.kddi-research.jp/sites/default/files/kddi_whitepaper_en/pdf/KDDI_B5G6G_WhitePaperEN_2.0.1.pdf

[7] "Beyond 5G white paper: Message to the 2030s, version 1.0." Beyond 5G Promotion Consortium, Kyoto, Japan, White Paper, Mar. 2022. [Online]. Available: https://b5g.jp/doc/whitepaper_en_1-0.pdf

[8] H. Q. Ngo, A. Ashikhmin, H. Yang, E. G. Larsson, and T. L. Marzetta, "Cell-free massive MIMO: Uniformly great service for everyone," in *Proc. IEEE 16th Int. Workshop Signal Process. Adv. Wireless Commun. (SPAWC)*, 2015, pp. 201–205.

[9] E. Nayebi, A. Ashikhmin, T. L. Marzetta, and H. Yang, "Cell-free massive MIMO systems," in *Proc. 49th Asilomar Conf. Signals Syst. Comput.*, 2015, pp. 695–699.

[10] S. Buzzi and C. D'Andrea, "User-centric communications versus cell-free massive MIMO for 5G cellular networks," in *Proc. 21th Int. ITG Workshop Smart Antennas*, 2017, pp. 1–6.

[11] Y. Hu, F. Zhang, C. Li, Y. Wang, and R. Zhao, "Energy efficiency resource allocation in downlink cell-free massive MIMO system," in *Proc. Int. Symp. Intell. Signal Process. Commun. Syst. (ISPACS)*, 2017, pp. 878–882.

[12] T. Okuyama, S. Suyama, J. Mashino, and Y. Okumura, "5G distributed massive MIMO with ultra-high density antenna deployment in low SHF bands," *IEICE Trans. Commun.*, vol. E100.B, no. 10, pp. 1921–1927, 2017.

[13] Z. Chen and E. Björnson, "Channel hardening and Favorable propagation in cell-free massive MIMO with stochastic geometry," *IEEE Trans. Commun.*, vol. 66, no. 11, pp. 5205–5219, Nov. 2018.

[14] T. Choi, P. Luo, A. Ramesh, and A. F. Molisch, "Co-located vs distributed vs semi-distributed MIMO: Measurement-based evaluation," in *Proc. 54th Asilomar Conf. Signals Syst. Comput.*, 2020, pp. 836–841.

[15] M. Ito *et al.*, "Effect of antenna distribution on spectral and energy efficiency of cell-free massive MIMO," in *Proc. IEEE 94th Veh. Technol. Conf. (VTC-Fall)*, 2021, pp. 1–5.

[16] L. D. Nguyen, H. D. Tuan, and T. Q. Duong, "Energy-efficient signalling in QoS constrained heterogeneous networks," *IEEE Access*, vol. 4, pp. 7958–7966, 2016.

[17] L. D. Nguyen, T. Q. Duong, H. Q. Ngo, and K. Tourki, "Energy efficiency in cell-free massive MIMO with zero-forcing precoding design," *IEEE Commun. Lett.*, vol. 21, no. 8, pp. 1871–1874, Aug. 2017.

[18] M. Alonzo, S. Buzzi, A. Zappone, and C. D'Elia, "Energy-efficient power control in cell-free and user-centric massive MIMO at millimeter wave," *IEEE Trans. Green Commun. Netw.*, vol. 3, no. 3, pp. 651–663, Sep. 2019.

[19] L.-N. Tran and H. Q. Ngo, "First-order methods for energy-efficient power control in cell-free massive MIMO: Invited paper," in *Proc. 53rd Asilomar Conf. Signals Syst. Comput.*, 2019, pp. 848–852.

[20] A. Zappone, E. Björnson, L. Sanguinetti, and E. Jorswieck, "Globally optimal energy-efficient power control and receiver design in wireless networks," *IEEE Trans. Signal Process.*, vol. 65, no. 11, pp. 2844–2859, Jun. 2017.

[21] M. Hmila, M. Fernández-Veiga, M. Rodríguez-Pérez, and S. Herrería-Alonso, "Energy efficient power and channel allocation in underlay device to multi device communications," *IEEE Trans. Commun.*, vol. 67, no. 8, pp. 5817–5832, Aug. 2019.

[22] M. W. Baidas, Z. Bahbahani, N. El-Sharkawi, H. Shehada, and E. Alsusa, "Joint relay selection and energy-efficient power allocation in downlink multi-cell NOMA networks," in *Proc. IEEE Wireless Commun. Netw. Conf. (WCNC)*, 2019, pp. 1–8.

[23] B. Su, Z. Qin, and Q. Ni, "Energy efficient uplink transmissions in LoRa networks," *IEEE Trans. Commun.*, vol. 68, no. 8, pp. 4960–4972, Aug. 2020.
[24] M. Ito *et al.*, "Evaluation on energy efficiency of UE in UL cell-free massive MIMO system with power control methods," in *Proc. IEEE GLOBECOM Workshops (GC Wkshps)*, 2021, pp. 1–6.
[25] T. Choi, M. Ito, I. Kanno, T. Oseki, K. Yamazaki, and A. F. Molisch, "Uplink energy efficiency of cell-free massive MIMO with transmit power control in measured propagation channels," in *Proc. IEEE Workshop Signal Process. Syst. (SiPS)*, 2021, pp. 164–169.
[26] T. Choi *et al.*, "Energy efficiency of uplink cell-free massive MIMO with transmit power control in measured propagation channel," *IEEE Open J. Circuits Syst.*, vol. 2, pp. 792–804, 2021.
[27] E. Dahlman, S. Parkvall, and J. Sköld, *5G NR: The Next Generation Wireless Access Technology*, 2nd ed. Amsterdam, The Netherlands: Academic, Sep. 2020.
[28] E. Nayebi, A. Ashikhmin, T. L. Marzetta, and B. D. Rao, "Performance of cell-free massive MIMO systems with MMSE and LSFD receivers," in *Proc. 50th Asilomar Conf. Signals Syst. Comput.*, 2016, pp. 203–207.
[29] M. Bashar, K. Cumanan, A. G. Burr, H. Q. Ngo, E. G. Larsson, and P. Xiao, "Energy efficiency of the cell-free massive MIMO uplink with optimal uniform quantization," *IEEE Trans. Green Commun. Netw.*, vol. 3, no. 4, pp. 971–987, Dec. 2019.
[30] J. Zhang, Y. Wei, E. Björnson, Y. Han, and X. Li, "Spectral and energy efficiency of cell-free massive MIMO systems with hardware impairments," in *Proc. 9th Int. Conf. Wireless Commun. Signal Process. (WCSP)*, 2017, pp. 1–6.
[31] Y. Zhang, H. Cao, M. Zhou, and L. Yang, "Power optimization for energy efficiency in cell-free massive MIMO with ZF receiver," in *Proc. 21st Int. Conf. Adv. Commun. Technol. (ICACT)*, 2019, pp. 366–371.
[32] Y. Zhang, Y. Cheng, M. Zhou, L. Yang, and H. Zhu, "Analysis of uplink cell-free massive MIMO system with mixed-ADC/DAC receiver," *IEEE Syst. J.*, vol. 15, no. 4, pp. 5162–5173, Dec. 2021.
[33] M. Bashar, K. Cumanan, A. G. Burr, M. Debbah, and H. Q. Ngo, "On the uplink max-min SINR of cell-free massive MIMO systems," *IEEE Trans. Wireless Commun.*, vol. 18, no. 4, pp. 2021–2036, Apr. 2019.
[34] M. C. Grant and S. P. Boyd. "CVX: MATLAB software for disciplined convex programming, version 2.2." Jan. 2020. [Online]. Available: http://cvxr.com/cvx/
[35] M. C. Grant and S. P. Boyd, "Graph implementations for nonsmooth convex programs," in *Recent Advances in Learning and Control*, V. D. Blondel, S. P. Boyd, and H. Kimura, Eds. London, U.K.: Springer, 2008, pp. 95–110. [Online]. Available: https://link.springer.com/chapter/10.1007/978-1-84800-155-8_7
[36] T. H. Nguyen, T. K. Nguyen, H. D. Han, and V. D. Nguyen, "Optimal power control and load balancing for uplink cell-free multi-user massive MIMO," *IEEE Access*, vol. 6, pp. 14462–14473, 2018.
[37] S. He, Y. Huang, L. Yang, B. Ottersten, and W. Hong, "Energy efficient coordinated beamforming for multicell system: Duality-based algorithm design and massive MIMO transition," *IEEE Trans. Commun.*, vol. 63, no. 12, pp. 4920–4935, Dec. 2015.
[38] "Spatial channel model for multiple input multiple output (MIMO) simulations (release 16)," 3GPP, Sophia Antipolis, France, Rep. TR 25.996 V16.0.0, Jul. 2020.
[39] Ö. T. Demir and E. Björnson, "Joint power control and LSFD for wireless-powered cell-free massive MIMO," *IEEE Trans. Wireless Commun.*, vol. 20, no. 3, pp. 1756–1769, Mar. 2021.
[40] Ö. Özdogan, E. Björnson, and J. Zhang, "Performance of cell-free massive MIMO with Rician fading and phase shifts," *IEEE Trans. Wireless Commun.*, vol. 18, no. 11, pp. 5299–5315, Nov. 2019.
[41] E. Björnson and L. Sanguinetti, "Scalable cell-free massive MIMO systems," *IEEE Trans. Commun.*, vol. 68, no. 7, pp. 4247–4261, Jul. 2020.
[42] E. Björnson, J. Hoydis, and L. Sanguinetti, "Massive MIMO networks: Spectral, energy, and hardware efficiency," *Found. Trends Signal Process.*, vol. 11, nos. 3–4, pp. 154–655, 2017. [Online]. Available: http://dx.doi.org/10.1561/2000000093
[43] T. L. Marzetta, "Noncooperative cellular wireless with unlimited numbers of base station antennas," *IEEE Trans. Wireless Commun.*, vol. 9, no. 11, pp. 3590–3600, Nov. 2010.

MASAAKI ITO received the B.S. and M.S. degrees in wireless communications from Waseda University, Tokyo, Japan, in 2016 and 2018, respectively.

From 2018 to 2019, he was a Staff with KDDI Corporation, Tokyo, Japan, and was engaged in mobile network operation. He is currently a Core Researcher with Wireless Communications System Laboratory, KDDI Research, Inc., Saitama, Japan. He is also been a Visiting Researcher with the University of Southern California, Los Angles, CA, USA, since 2021. His main research topic is user-centric networks.

ISSEI KANNO received the Ph.D. degree from the Tokyo Institute of Technology, Tokyo, Japan, in 2008.

He then joined KDDI Corporation, where he has been engaged in research on software defined radio, antennas, and propagation in mobile communication systems. From 2013 to 2015, he was engaged in research on cognitive radio with the Advanced Telecommunications Research Institute International. Since 2015, he has been engaged in research on wireless communication systems, including 5G and beyond with KDDI Research Inc. His current research interests include signal processing and resource utilization for wireless communication systems.

Dr. Kanno received the Best Paper Award at IEEE WCNC 2010 from IEEE, the Young Researcher's Award, and the Distinguished Service Award from IEICE in 2012.

KOSUKE YAMAZAKI received the Ph.D. degree from Tokyo University, Japan, in 2005.

He joined KDDI and engaged in the research and development on software defined radio, cognitive radio, WiMAX, Wi-Fi, and heterogeneous networks. Since 2022, he has been an Expert, Wireless Technology Division, Advanced Technology Laboratories, KDDI Research, Inc.

Dr. Yamazaki received the Young Researcher's Award and the Distinguished Contributions Award from IEICE in 2010 and 2018, respectively.

YOJI KISHI received the B.S. and M.S. degrees in electrical engineering from Kyoto University, Kyoto, Japan, in 1989 and 1991, respectively.

He joined Kokusai Denshin Denwa Company Ltd. (currently KDDI Corporation) in 1991, where he has been engaged in research and development on the operation planning of telecommunications networks. He has been an Executive Director with KDDI Research, Inc., since 2016 and Leads research and development activities toward beyond 5G and 6G.

Mr. Kishi received the Young Researcher's Award from IEICE and the Meritorious Award on Radio from the Association of Radio Industries and Businesses in 1998 and 1999.

WEI-YU CHEN received the B.S. degree from the Department of Electrical Engineering, National Dong Hwa University, Hualien, Taiwan, in 2014, and the M.S. degree from the Department of Electrical Engineering, National Tsing Hua University, Hsinchu, Taiwan, in 2016. He is currently pursuing the Ph.D. degree with the Ming Hsieh Department of Electrical and Computer Engineering, University of Southern California, Los Angeles, USA.

His current research interests include performance analysis and algorithm design for cell-free massive MIMO wireless systems, mobile edge computing networks, and next-generation wireless communication systems.

THOMAS CHOI (Graduate Student Member, IEEE) received the B.S. degree in electrical engineering from the University of Southern California (USC) in 2015, the first M.S. degree in aerospace engineering from the Georgia Institute of Technology in 2017, and the second M.S. degree in electrical engineering from USC in 2020, where he is currently pursuing the Ph.D. degree in electrical and computer engineering.

His main research interest is verifying performances of massive MIMO technologies based on actual measured channel data, especially in the areas of distributed MIMO systems, UAV applications, and channel extrapolation.

ANDREAS F. MOLISCH (Fellow, IEEE) received the Dipl.Ing., Ph.D., and Habilitation degrees from Technical University Vienna, Austria, in 1990, 1994, and 1999, respectively.

He spent the next ten years in industry, with FTW, AT&T (Bell) Laboratories, and Mitsubishi Electric Research Labs (where he rose to Chief Wireless Standards Architect). In 2009, he joined the University of Southern California, Los Angeles, CA, USA, where he is currently the Solomon Golomb-Andrew and Erna Viterbi Chair Professor. He has authored five books, more than 300 journal papers, numerous conference papers, and more than 70 patents. He is a Clarivate Highly Cited Author, with h-index >100. His main research interests are wireless propagation channels, multi-antenna systems, localization, machine learning, novel modulation formats, edge computing, and caching.

Dr. Molisch is a recipient of numerous awards. He is a Fellow of NAI, AAAS, and IET and a member of the Austrian Academy of Sciences.